



# White Light Emitting Transparent Double Layer Stack of $\text{Al}_2\text{O}_3:\text{Eu}^{3+}$ , $\text{Tb}^{3+}$ , and $\text{Ce}^{3+}$ Films Deposited by Spray Pyrolysis

S. Carmona-Télez,<sup>a,z</sup> C. Falcony,<sup>a</sup> M. Aguilar-Frutis,<sup>b</sup> G. Alarcón-Flores,<sup>b</sup> M. García-Hipólito,<sup>c</sup> and R. Martínez-Martínez<sup>d</sup>

<sup>a</sup>CINVESTAV-IPN, México D.F. 07360, México

<sup>b</sup>CICATA-IPN, México D.F. 11500, México

<sup>c</sup>IIM-UNAM, México D.F. 04510, México

<sup>d</sup>IFM-UTM, Oaxaca 69000, México

Aluminum oxide films doped with Tb, Ce and Eu have been deposited by spray pyrolysis using acetylacetonates as precursors. The photoluminescence emission for these films and for double layer stacks is reported. Eu and Tb doped films present the emissions associated with the radiative transitions among the electronic energy states of the triple ionized atom, being dominant the  $^5\text{D}_0$  to  $^7\text{F}_2$  at  $\sim 612.5$  nm for the  $\text{Eu}^{3+}$  ion, and the  $^5\text{D}_4$  to  $^7\text{F}_5$  at  $\sim 547.5$  nm for the  $\text{Tb}^{3+}$  ion. In the case of Ce doped films, there are two broad bands associated also with the 5d to 4f transitions of this ion at  $\sim 400$  and 510 nm. These films have low surface roughness lower than 3 nm, and thickness between 50 to 260 nm. The double layer stacks involved an initial Eu doped layer and a second Ce and Tb co-doped layer with different thicknesses. The films are transparent with an optical bandgap of approximately 5.63 eV, the photoluminescence of these stacks presented an overlap of the emissions corresponding to all the dopants when excited with 300 nm light, resulting in a white light emission.

© 2013 The Electrochemical Society. [DOI: 10.1149/2.017306jss] All rights reserved.

Manuscript submitted January 30, 2013; revised manuscript received April 23, 2013. Published May 3, 2013.

The physical and chemical properties of aluminum oxide are attractive for different types of applications; this is the case of dosimetry, where aluminum oxide has been used to make ionizing and nonionizing radiation sensors.<sup>1,2</sup> Microelectronics is another example as  $\text{Al}_2\text{O}_3$  is considered a good high-K dielectric for CMOS and for new generation memory devices.<sup>3,4</sup> Also  $\text{Al}_2\text{O}_3$ , among other metallic oxides, doped with rare earths has been found to be a good luminescent material.<sup>5-11</sup> This is the case of  $\text{Al}_2\text{O}_3:\text{Eu}^{3+},\text{Tb}^{3+}$  and  $\text{Ce}^{3+}$  films synthesized by the spray pyrolysis technique,<sup>12-14</sup> where besides an intrinsic emission from localized states in the  $\text{Al}_2\text{O}_3$  host at 415 nm, the luminescent emissions related to transitions between electronic energy levels of the rare earth ions are observed. When  $\text{Eu}^{3+}$  ions are introduced in these films, a charge transfer mechanism to these ions from the localized states in the aluminum oxide host has been reported to occur rendering an increase of the luminescence intensity and an extended luminescence decay time compared to those observed when the excitation is produced through an inter-electronic energy level transition in the  $\text{Eu}^{3+}$  ion.<sup>11</sup> Tunability of light emission has become an active area for luminescent materials synthesis in recent years for applications such as white light emitting solid state devices, this can be achieved by different methods, one is by co-doping with different luminescent centers,<sup>15</sup> another one is by overlapping the emission of multiple layers. Aluminum oxide has been reported to be one of the materials used in the first approach<sup>15,16</sup> by a ternary doping with Ce, Tb and Mn each contributing with light emissions in the blue, green and red respectively.  $\text{Al}_2\text{O}_3$  thin films have been deposited by a wide variety of techniques such as laser ablation,<sup>17</sup> sputtering,<sup>18</sup> atomic layer deposition,<sup>19</sup> metal organic chemical vapor deposition (MOCVD)<sup>20,21</sup> and others. Spray pyrolysis<sup>22-27</sup> is a simple atmospheric pressure technique, which is easily scalable to industrial level for an eventual synthesis of large area films. For some applications like electroluminescent devices a serious consideration has to be given to transparency and surface roughness, the use of inorganic precursor in spray pyrolysis technique has been documented to lead to the formation of opaque films with high roughness.<sup>16</sup> The use of organic precursor for aerosol generation in the spray pyrolysis deposition of films results in homogeneous materials with high planarity.<sup>28</sup> This work was focused on obtaining low roughness; transparent films doped with rare earths that show luminescence in the three basic colors. For this purpose single doped films and double layer stacks of a Ce and Tb co-doped film on top of an Eu doped film deposited by spray pyrolysis were studied for different doping concentrations and

thicknesses of the double layer stack. The reason for this separation was that the highest emission intensity for the Eu ion was achieved at a different deposition temperature than that needed for the optimum emission of Ce and Tb ions. The chromaticity coordinates were also determined for these samples.

## Experimental

Aluminum, Cerium, Europium, and Terbium acetylacetonates dissolved in N-N dimethylformamide were used as spraying solution in this work. The ultrasonic spray pyrolysis technique used in this work consists in generating by ultrasonic means an aerosol from a spraying solution of the precursor reactants which is carried through a nozzle directly to a hot substrate where undergoes a pyrolytic decomposition to form a solid film or coating on top of the substrate.<sup>22</sup> For each dopant it was necessary to optimize the deposition conditions. In every case a 0.92 M solution of aluminum acetylacetonate in N,N-Dimethylformamide was used. Tb doped films were synthesized adding 5, 7, 10 y 15 atomic percent of terbium acetylacetonate [ $\text{Tb}(\text{acac})_3$ ] to the aluminum in the spraying solution, at a temperature between 400 to 550°C. In the case of  $\text{Al}_2\text{O}_3:\text{Eu}^{3+}$  thin films, were used 1, 3, 5, 7 and 10 atomic percent of  $\text{Eu}(\text{acac})_3$ , at a temperature of 450 to 600°C. Finally  $\text{Al}_2\text{O}_3:\text{Ce}^{3+}$  thin films were synthesized using 0.25, 0.5, 1, 1.5, 2, 3 and 5 atomic percent of  $\text{Ce}(\text{acac})_3$  in the spraying chemical solution, and a temperature between 400 to 500°C. Using the results obtained for the single layers, the relative doping concentrations used on the double layer stacks were fixed as follows; first a film with 10% concentration of  $\text{Eu}(\text{acac})_3$  in the spraying solution was deposited at 600°C for 14 minutes. The second layer incorporated 2% Ce and 7% Tb in the starting solution and was deposited in the 5 to 8 minutes range at 435°C. The reproducibility of the luminescent characteristics of the films was within a 5% variation in all cases. Pieces of silicon wafers (111 and 100) of about  $\sim 1$  cm<sup>2</sup> were used as substrates. Dry air was used as carrier gas. Refraction index and thickness measurements on the films were made using a Gaertner LSE Stokes Ellipsometer (632.8 nm), roughness and morphology were measured with an Atomic Force Microscope Veeco CP Research, EDS analysis were measured in a Scanning Electron Microscope JEOL using an acceleration voltage of 3 KV. Finally photoluminescence measurements were carried out using a SPEX Fluoro-Max-P spectrophotometer. All measurements were carried out at room temperature.

## Results and Discussion

Fig. 1 shows atomic force microscopy (AFM) images for A)  $\text{Al}_2\text{O}_3$  films doped with 7% of Tb; B)  $\text{Al}_2\text{O}_3$  films doped with 2% Ce; C)

<sup>z</sup>E-mail: arribalarevolucion@hotmail.com

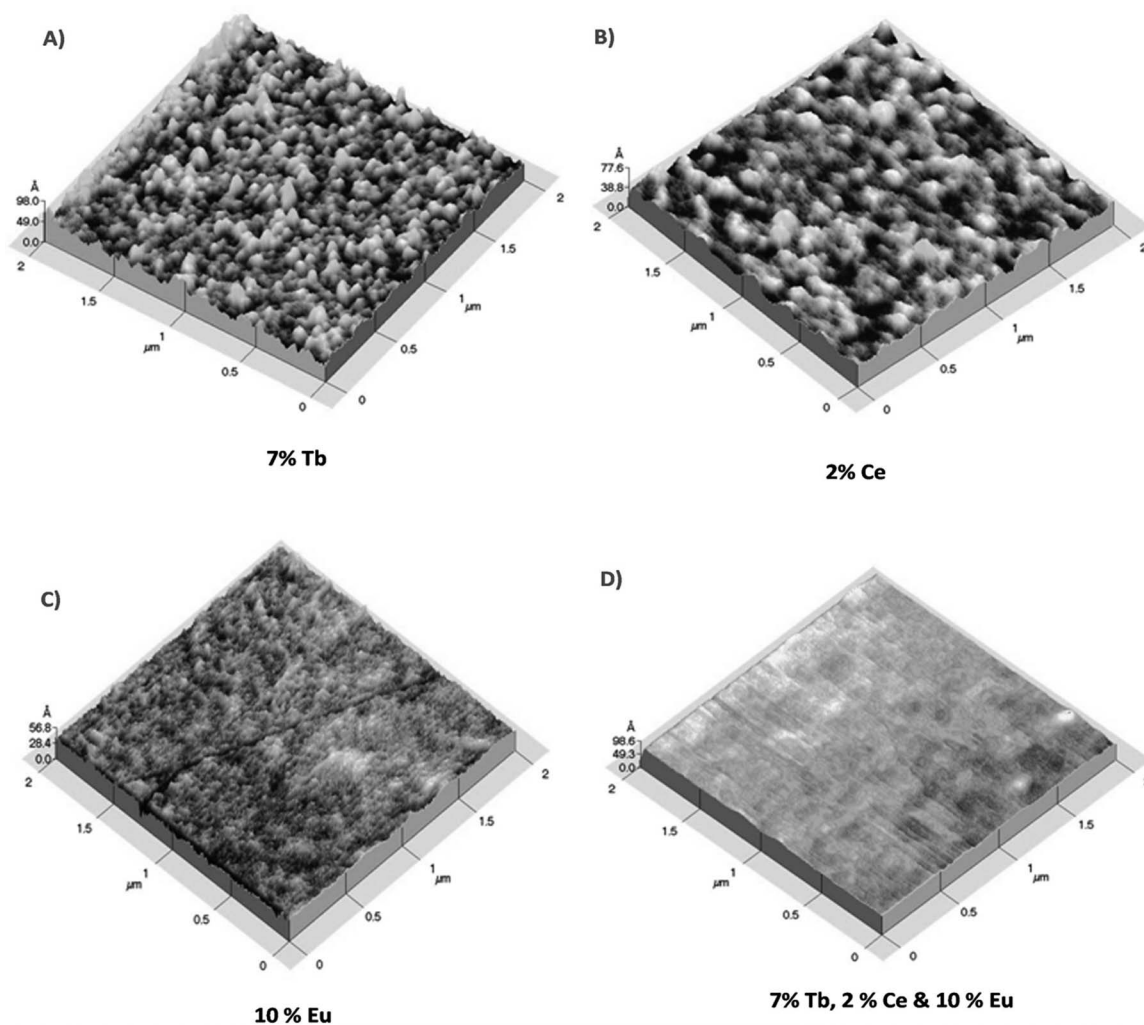


**Figure 1.** AFM images: A)  $\text{Al}_2\text{O}_3$  films doped with 7% of Tb; B)  $\text{Al}_2\text{O}_3$  films doped with 2% Ce; C)  $\text{Al}_2\text{O}_3$  films doped with 10% Eu; and D)  $\text{Al}_2\text{O}_3$  films doped with 10% of Eu, 7% of Tb, and 2% of Ce.

$\text{Al}_2\text{O}_3$  films doped with 10% Eu, and D)  $\text{Al}_2\text{O}_3$  films doped with 10% of Eu, 7% of Tb and 2% of Ce. These surfaces are planar, with low roughness (RMS less than 3 nm) for all cases including multiple doped films. The low roughness values are expected when metal-organic compounds are used as precursors and can be explained by analyzing the growth kinetics involved in the spray pyrolysis deposition process of the films in which the relatively low evaporation temperatures of these compounds create a chemical vapor deposition (CVD) type of growth on the substrate surface.<sup>28</sup> In this scheme an excellent coverage of the substrate surface is achieved which provides a film surface rather flat, uniform and with low surface roughness, unlike films deposited with precursors based on nitrates, chlorides or fluorides that render opaque films with powder or granular growth and large surface roughness.<sup>29</sup> Low surface roughness is of major importance when the luminescent films are to be integrated in multilayer electroluminescence devices.

Table I lists EDS the relative atomic percent elemental compositions of the RE (europium, cerium or terbium), aluminum and oxygen concentrations in the single doped films. The doping concentration in the spraying solution and the deposition temperature for each film are also listed, these films presented the highest luminescent emission. In general the incorporation efficiency of each dopant is quite different, thus the percent content of the dopant in the spraying solution must be adjusted in order to incorporate similar amount of dopant in each type of film. There is also an excess of oxygen in the films compared

with the expected stoichiometry for  $\text{Al}_2\text{O}_3$  which may indicate a low density material.

Table II shows the values of the thicknesses and refractive index of the single doped films and for the double layer stack, as determined by single wavelength ellipsometry at 630 nm, for the best luminescent samples. Also, the deposition rate and deposition time as well as the dopant percent in the spraying solution are listed in this table.

The relatively low deposition rates and low refractive index values are evident from this table. Deposition rates up to 30 Å/s. and refractive index close to 1.7 have been reported for aluminum oxide films deposited with a second aerosol stream of a 1:1  $\text{H}_2\text{O}$  and  $\text{NH}_4\text{OH}$  solution.<sup>30</sup> However, the light emission intensity of RE-doped films is dramatically decreased, if a similar approach is used. Thus, the material obtained in this work is porous and less dense than that previously reported.

**Table I.** Atomic percent content of oxygen, aluminum, europium, cerium, and terbium as measured by EDS on the single doped films.

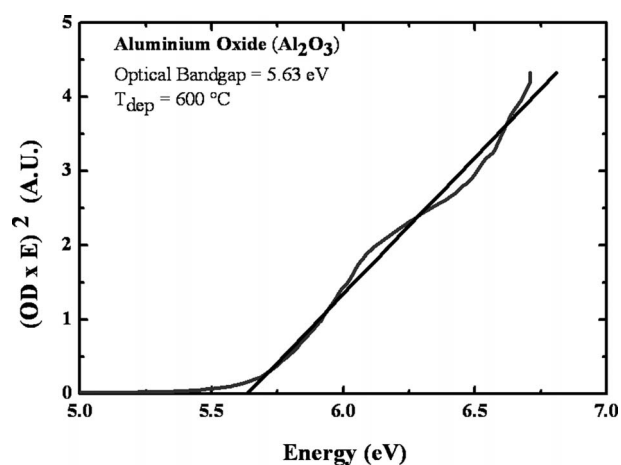
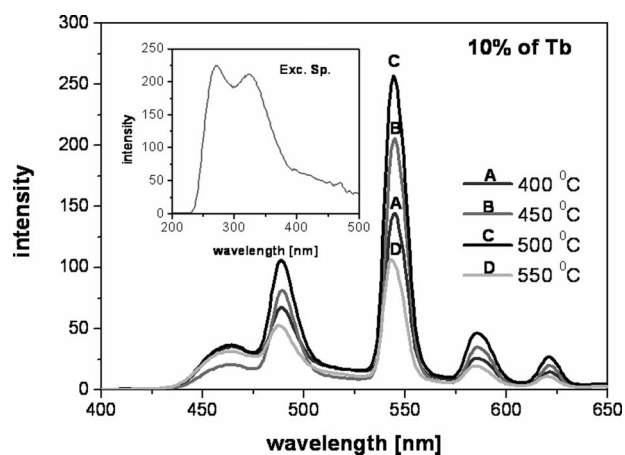
Kind of Sample	TR <sup>3+</sup> (%)	T(°C)	EDS (a/o)			
			TR <sup>3+</sup>	O	Al	R(O/Al)
$\text{Al}_2\text{O}_3:\text{Eu}$	7%	550	0.82	70.04	29.14	2.4
$\text{Al}_2\text{O}_3:\text{Ce}$	2%	435	0.67	60.18	39.15	1.53
$\text{Al}_2\text{O}_3:\text{Tb}$	10%	450	0.59	74.99	24.42	3.1

**Table II.** The values of the thicknesses and refractive index of the single doped films and for the double layer stack are shown.

Sample	Thickness (Å)	time (s)	Deposition rate (Å/s)	Refractive index	
Al <sub>2</sub> O <sub>3</sub> :Eu at 550°C	7%	2677 ± 50	600	4.5 ± 0.4	1.679 ± 0.003
Al <sub>2</sub> O <sub>3</sub> :Ce at 435°C	2%	847 ± 20	600	1.4 ± 0.2	1.606 ± 0.004
Al <sub>2</sub> O <sub>3</sub> :Tb at 450°C	10%	1792 ± 45	600	3.0 ± 0.2	1.601 ± 0.001
Al <sub>2</sub> O <sub>3</sub> Double layer, step 1 at 600°C step 2 at 435°C	10% Eu, 2% Ce y 7% Tb	3523 ± 72	Step 1: 840 Step 2: 300 Total: 1140	3.1 ± 0.9	1.614 ± 0.014

Fig. 2 shows the UV-Vis characteristics for Al<sub>2</sub>O<sub>3</sub> thin films deposited at 600°C by ultrasonic spray pyrolysis using aluminum acetylacetonate as precursor material.<sup>26</sup> This plot presents the square of the optical absorption times the photon energy as a function of photon energy. From this plot it is possible to determine the optical energy bandgap for these films. In this case the bandgap is equal to 5.63 eV. It is observed that these films are transparent in the whole visible range, and comparable to the best quality films obtained by other techniques.<sup>31</sup> Since the luminescent centers in the film have to be efficiently excited and the photoluminescence collected, the transparency of the films to the excitation and emission wavelengths is a highly appreciated characteristic.

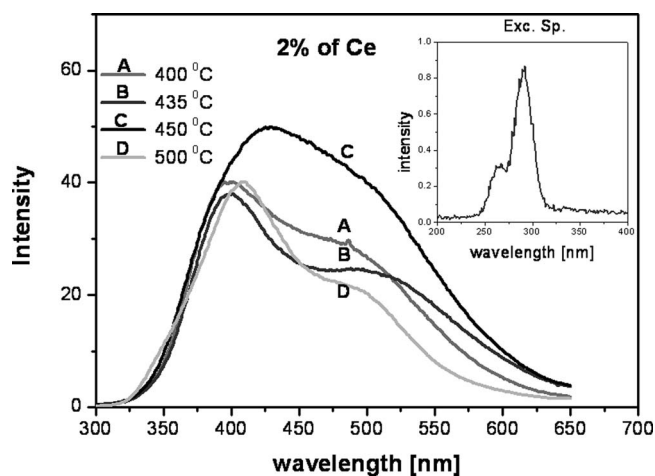
The photoluminescence spectra for Tb<sup>3+</sup>-doped Al<sub>2</sub>O<sub>3</sub> films are shown in Fig. 3, for 10% Terbium content in the spraying solution, synthesized at 400, 450, 500 and 550°C. The luminescence peaks observed are associated with inter-level transitions within the electronic

**Figure 2.** UV-Vis characteristics for Al<sub>2</sub>O<sub>3</sub> thin films deposited at 600°C.**Figure 3.** PL spectra for Tb-doped films for 10% Terbium content, synthesized at 400 to 550°C, excitation wavelength used was 271 nm. The excitation spectrum for the 545 nm peak is shown at inset.

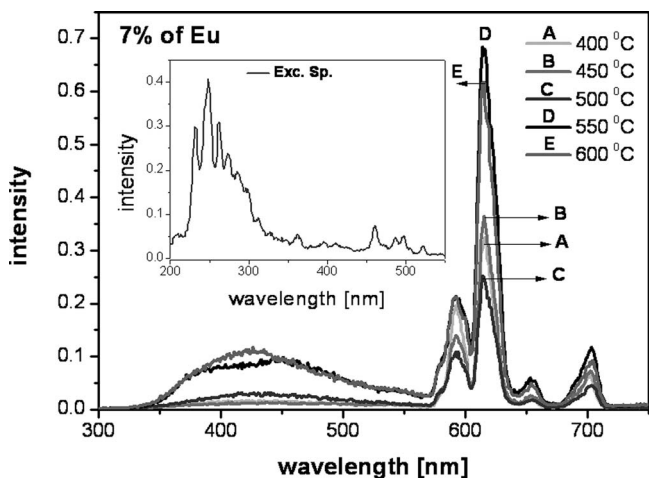
energy states of Tb<sup>3+</sup> ions, particularly those corresponding to transitions among levels <sup>5</sup>D<sub>4</sub> to <sup>7</sup>F<sub>6</sub>, <sup>7</sup>F<sub>5</sub>, <sup>7</sup>F<sub>4</sub> and <sup>7</sup>F<sub>3</sub>, located at 490, 545, 590, and 622 nm respectively. The dominant peak for these spectra is the one associated with the transition <sup>5</sup>D<sub>4</sub> to <sup>7</sup>F<sub>5</sub> at 545 nm, which gives the characteristic green light emission identified with the presence of Tb<sup>3+</sup> ions. The mayor light emission intensity is obtained for 10% Tb content, larger concentrations result in a luminescence quenching effect associated with energy transfer among dopant ions. The general behavior of these results is similar to that reported previously<sup>12</sup> in which a dependence of the photoluminescence intensity is correlated with the incorporation efficiency of the Tb ions into the aluminum oxide matrix, in the present case the maximum is observed at 500°C. The inset in this figure shows the excitation spectrum for the dominant luminescent peak in the 200 to 400 nm range, a double excitation peaks are observed at ~ 271 and 325 nm respectively, corresponding to (<sup>7</sup>F<sub>6</sub> to <sup>5</sup>H<sub>5</sub>, <sup>5</sup>H<sub>6</sub>) and (<sup>7</sup>F<sub>6</sub> to <sup>5</sup>H<sub>7</sub>, <sup>5</sup>D<sub>1</sub>) transitions of the Tb<sup>3+</sup> ion. In order to achieve these spectra a 271 nm excitation wavelength was used.

Fig. 4 shows the photoluminescence spectra of Al<sub>2</sub>O<sub>3</sub>:Ce<sup>3+</sup> films doped with 2% of cerium deposited at 400, 435, 450 and 500°C, the excitation wavelength used was 290 nm. The luminescence spectra peaks observed are broad and they are located at approximately 400 and 500 nm, they seem to be associated with inter-level transitions of the electronic energy states of Ce<sup>3+</sup> (5d→4f emission of Ce<sup>3+</sup> ions). It is appreciated that the largest emission intensity is obtained at 450°C. The inset shows the excitation spectrum for the 480 nm emission peak. There is a dominant excitation peak at 290 nm. These results are similar to those previously reported for the luminescent properties of Al<sub>2</sub>O<sub>3</sub>:Ce films synthesized by spray pyrolysis using aluminum and cerium chlorides as precursors.<sup>15,16</sup> This is the first report of luminescent Ce doped aluminum oxide synthesized with acetylacetonates as raw precursors by the ultrasonic spray pyrolysis technique.

Fig. 5 shows the photoluminescent spectra of Al<sub>2</sub>O<sub>3</sub>:Eu<sup>3+</sup>, using a doping concentration of 7% and temperatures in the range from 400 to 600°C. The luminescence spectra peaks observed are associated with

**Figure 4.** PL spectra of Al<sub>2</sub>O<sub>3</sub>:Ce films for 2% of cerium content, deposited at 400 to 500°C, the excitation wavelength used was 290 nm. The inset shows the excitation spectrum for the 480 nm emission peak.





**Figure 5.** PL spectra of  $\text{Al}_2\text{O}_3:\text{Eu}^{3+}$ , using a doping concentration of 7% and a temperature range from 400 to 600 °C, a 248 nm excitation wavelength was used to obtain these spectra.

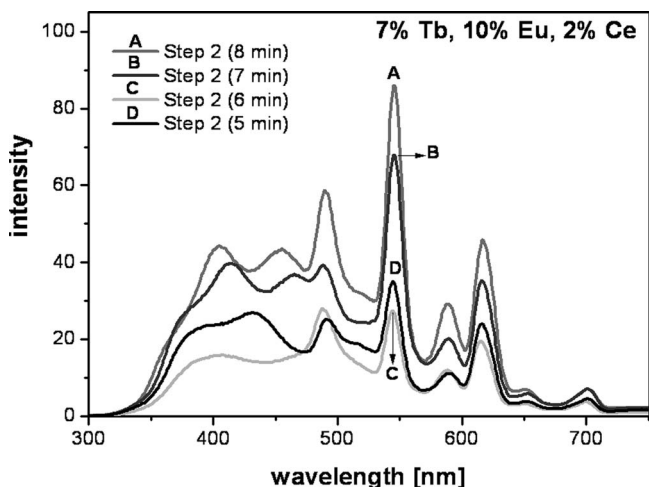


**Figure 6.** PL spectra of a double layer stack of  $\text{Al}_2\text{O}_3$  with 10% of Eu / 7% of Tb and 2% Ce, for different send step deposition times. The excitation wavelength to generate these spectra was 300 nm.

inter level transitions within the electronic energy states of  $\text{Eu}^{3+}$  ions, particularly those associated with transitions levels  $^5\text{D}_0$  to  $^7\text{F}_1$ ,  $^7\text{F}_2$ ,  $^7\text{F}_3$  y  $^7\text{F}_4$ , and they are located at 590, 612, 650, and 697 nm, respectively. All spectra show similar emission characteristics displaying a dominant peak associated with the transition  $^5\text{D}_0$  to  $^7\text{F}_2$  at 612 nm, so that; the light emission is predominantly red. It is appreciated that the highest light emission intensity is obtained in the films deposited at a substrate temperature of 550°C. These spectra were generated with a 248 nm excitation wavelength corresponding to the excitation peak presented in Fig. 5 inset. These results are similar to those previously reported for aluminum oxide doped with europium, synthesized with chloride raw precursors, it was found that the best light emission intensity was achieved using 20% of doping concentration and deposited at 600°C.<sup>32</sup>

Fig. 6 shows the photoluminescent spectra of a double layer stack of  $\text{Al}_2\text{O}_3$  with 10% of Eu, 7% of Tb and 2% Ce. This type of sample was designed with the purpose of producing a white light emission, thus the doping concentrations and the relative thickness of the layers were adjusted with this aim in mind. Since the optimal conditions for the luminescent characteristics of each dopant are not the same, the Eu doped film was deposited first at 600°C, and a Ce/Tb co-doped film was then deposited at 435°C. The spectra in this figure show the characteristic emission peaks for cerium, terbium and europium at 400 to 465 nm, 547.5 nm and at 612.5 nm respectively. In all cases, the presence of the three  $\text{RE}^{3+}$  are observed, but the relative intensity of their characteristic peaks is correlated with the thickness variation of the second layer. A 5 min. deposition time layer in step 2 generates a balanced emission of the different ions, producing an overall white light luminescence. In the remaining cases (longer deposition times), it is observed an increase in the emission intensity of the band centered at 547.5 nm ( $\text{Tb}^{3+}$ ), which leads to a blue green emission. The excitation wavelength to generate these spectra was 300 nm. Aluminum oxide white light emitting films, synthesized by spray pyrolysis using inorganic raw precursors, have already been reported using Ce, Tb and Mn instead of Eu as dopants (simultaneous incorporation of Ce, Tb and Eu rendered poor results). However, these films presented high roughness morphology.<sup>33</sup> In the present case, the use of organic raw precursors is novel since it was possible to incorporate the three rare earth activator ions ( $\text{Ce}^{3+}$ ,  $\text{Tb}^{3+}$  and  $\text{Eu}^{3+}$ ) without the presence of  $\text{Cl}^-$  ions, and the films were homogeneous with an average roughness lower than 26 Å.

Fig. 7 part A) shows the diagram CIE (*Commission internationale de l'éclairage*),<sup>34</sup> which precisely defines the three primary colors of additive color synthesis, from which all others can be created, depending on its coordinates (x, y) individuals. The global emission

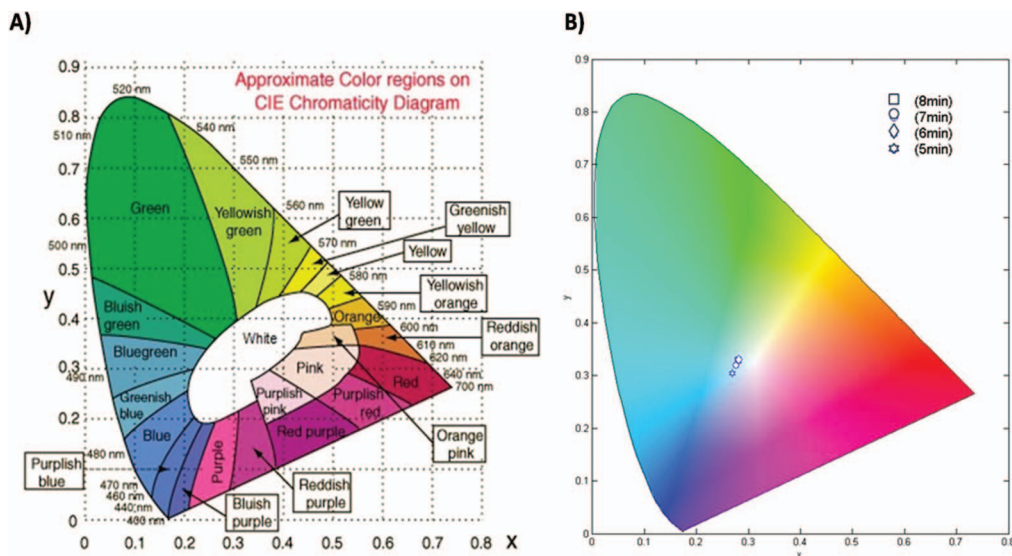


**Figure 7.** part A) CIE 1931 color space chromaticity diagram, part B) global emission generated from double layer stack films.

**Table III. Experimental CIE diagram corresponding coordinates are presented.**

Sample	X	Y
8 min	0.2798	0.3287
7 min	0.2751	0.3189
6 min	0.2812	0.3305
5 min	0.2692	0.3048

generated from triply doped thin films (excited using a wavelength of 300 nm) was characterized by its chromaticity coordinates in a CIE diagram, presented in Part B) of the previous image. Their corresponding coordinates are presented in Table III. According to the CIE diagram all cases fall in the “White” area, however, it is fair to point out that in all cases there is a tendency toward green, due to the dominant emission of Tb<sup>3+</sup> ions. These results are comparable to those reported previously using Ce, Tb and Mn.<sup>13</sup>

### Conclusions

Transparent and low average roughness luminescent aluminum oxide films have been synthesized through the use of metal-organic precursors incorporating Tb<sup>3+</sup>, Eu<sup>3+</sup> and Ce<sup>3+</sup> ions as luminescent activators. These films were deposited by the ultrasonic spray pyrolysis technique. In particular, luminescent films with the incorporation of Ce using organic precursors by this technique had not been reported previously. The novel double layer stack design allowed to incorporate Eu together with Ce and Tb in a white light emitting multilayer, achieving planar and homogeneous morphologies, typical of those films synthesized using organic materials as raw precursors. The characteristics of these films are suitable for potential use in electroluminescence applications.

### Acknowledgments

The authors wish to acknowledge the technical assistance of Z. Rivera, R. Fragoso, M. Guerrero and A. Soto from physics department of CINVESTAV-IPN; to Alfonso Martínez from CICATA-IPN

and E. Yescas-Mendoza from UTM. The authors also thank CONACYT and ICyT DF for financial support, as well as SIP-IPN Project No.20101556 and 20111101.

### References

1. P. Bilski and P. Olko, *Radiant Meas.*, **24**, 445 (1995).
2. J. Bhom, Dosimetry of weakly penetrating radiation PTB-Dos-30.
3. J. Robertson, *Rep. Prog. Phys.*, **69**, 327 (2006).
4. G. D. Wilk, *J. Appl. Phys.*, **89**, 5243 (2001).
5. S. L. Jones, *Appl. Phys. Lett.*, **71**, 404 (1997).
6. G. A. Hirata, *J. Vac. Sci. Tech. A*, **14**, 1 (1996).
7. Yuko Satoh, *Science and Technology of Advanced Materials*, **6**, 215 (2005).
8. E. Pereyra-Perea, *J. Phys. D*, **31**, L7 (1998).
9. C. Chacon-Roa, *Journal of Physics D: Applied Physics* (2007).
10. S. Bachir, Editor Blackwell Scientific Publication, Oxford, U. K. *J. Lumin.* **75**, 35 (1997).
11. E. F. Huerta and I. Padilla, *Optical Materials*, **34**, 1137 (2012).
12. A. E. Esparza-Garcia, *Journal of ECS*, **150**, H53 (2003).
13. R. Martínez-Martínez, *Thin Solid Films*, **325**, 14 (1998).
14. R. Martínez-Martínez, *Advances in Science and Technology*, **82**, 19 (2013).
15. R. Martínez-Martínez, *Thin Solid Films*, D09-00746 (2006).
16. R. Martínez-Martínez, *Nucl. Instr. and Meth. in Phys. Res. B*, **241**, 450 (2005).
17. Nikifor Rakov, *Appl. Phys. Lett.*, **83**, 272 (2003).
18. P. Jin, *J. Vac. Sci. Technol. A*, **20**, 2134 (2002).
19. Y. Kim, *Appl. Phys. Lett.*, **71**, 3604 (1997).
20. Davide Barreca, *J. Mater. Chem.*, **10**, 2127 (2000).
21. F. Wiest, *Thin Solid Films*, **496**, 240 (2006).
22. M. Langlet and J. C. Joubert, *Chemistry of advanced Materials*, C. N. R. Rao. Chemistry Advanced Materials, Blackwell Scientific Publications, Oxford, 1993.
23. C. Falcony, *J. Electrochem. Soc.*, **139**, 267 (1992).
24. C. Falcony and M. Garcia, *J. Electrochem. Soc.*, **141**, 2860 (1994).
25. M. Aguilar-Frutis, *Applied Physics Letters*, **72**, 14.
26. S. Carmona-Tellez and S. Aguilar-Frutis, *J. Appl. Phys.*, **103**, 034105 (2008).
27. S. Carmona Téllez, *ECS Transactions*, **25**(6), 179 (2009).
28. J. C. Vigué and J. Spitz, *J. Electrochem. Soc.: Solid-State Science and Technology*, **122**(4), 585 (1975).
29. G. Blandenet and Y. Lagarde, *Thin Solid Films*, **77**, 81 (1981).
30. S. Carmona-Téllez, tesis maestría CICATA-IPN (2008).
31. P. Patil, *Thin Solid Films*, **228**, 120 (1996).
32. A. E. Esparza-Garcia, *Superficies y Vacío*, **9**, 74 (1999).
33. R. Martínez-Martínez, *Journal of Materials Research Society*, **25**, 3 (2010).
34. Deane B. Judd and David L. Macadam, *Journal of Optical Society of America*, **54**, 1031 (1964).